SI Appendix for

Predicting tipping points in mutualistic networks through dimension reduction

J.-J. Jiang, Z.-G. Huang, T. P. Seager, W. Lin, C. Grebogi, A. Hastings, and Y.-C. Lai

October 25, 2017

Contents

SI Appendix figures

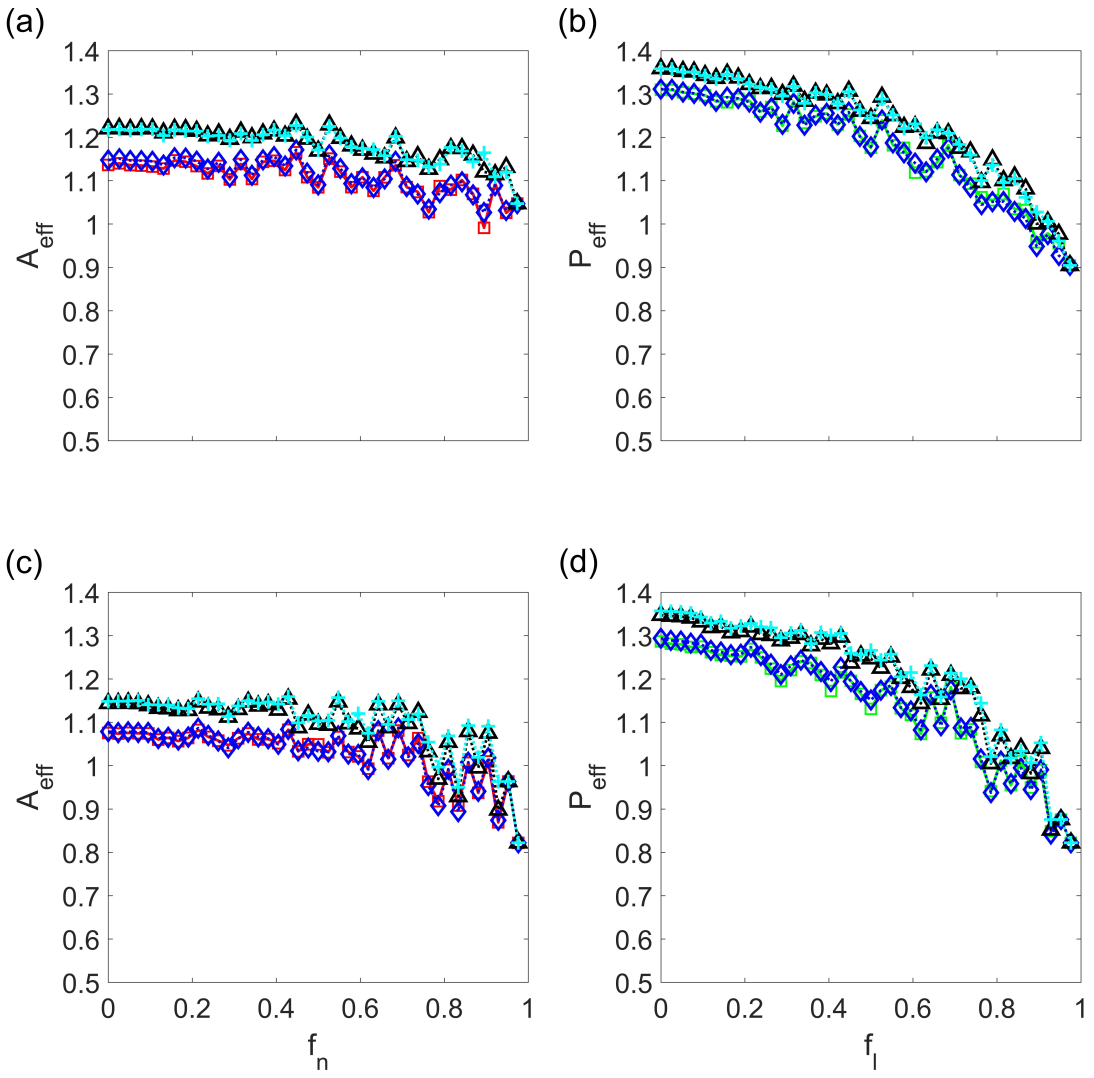

fig. S1. Representative resilient functions in systems that do not exhibit a tipping point. For networks A [panels (a,b)] and B [panels (c,d)], typical examples of resilient functions of pollinator abundance [panels (a,c)] versus f_n, the fraction of removed pollinators, and plant abundance [panels (b,d)] versus f_l, the fraction of removed mutualistic links corresponding to the value of f_n in panels (a,c). The curves with red squares are from the original networked system, while the curves with diamonds, triangles, and crosses are the corresponding individual resilient functions from reduced 2D model with averaging methods 1-3, respectively. The parameters are $h = 0.7$, $t = 0.5$, $\beta_{ii}^{(A)} = \beta_{ii}^{(P)} = 1$, $\alpha_i^{(A)} = \alpha_i^{(P)} = 0.3$, $\mu_A = \mu_P = 0.0001$, $\gamma_0 = 1$, and $\kappa = 0$.

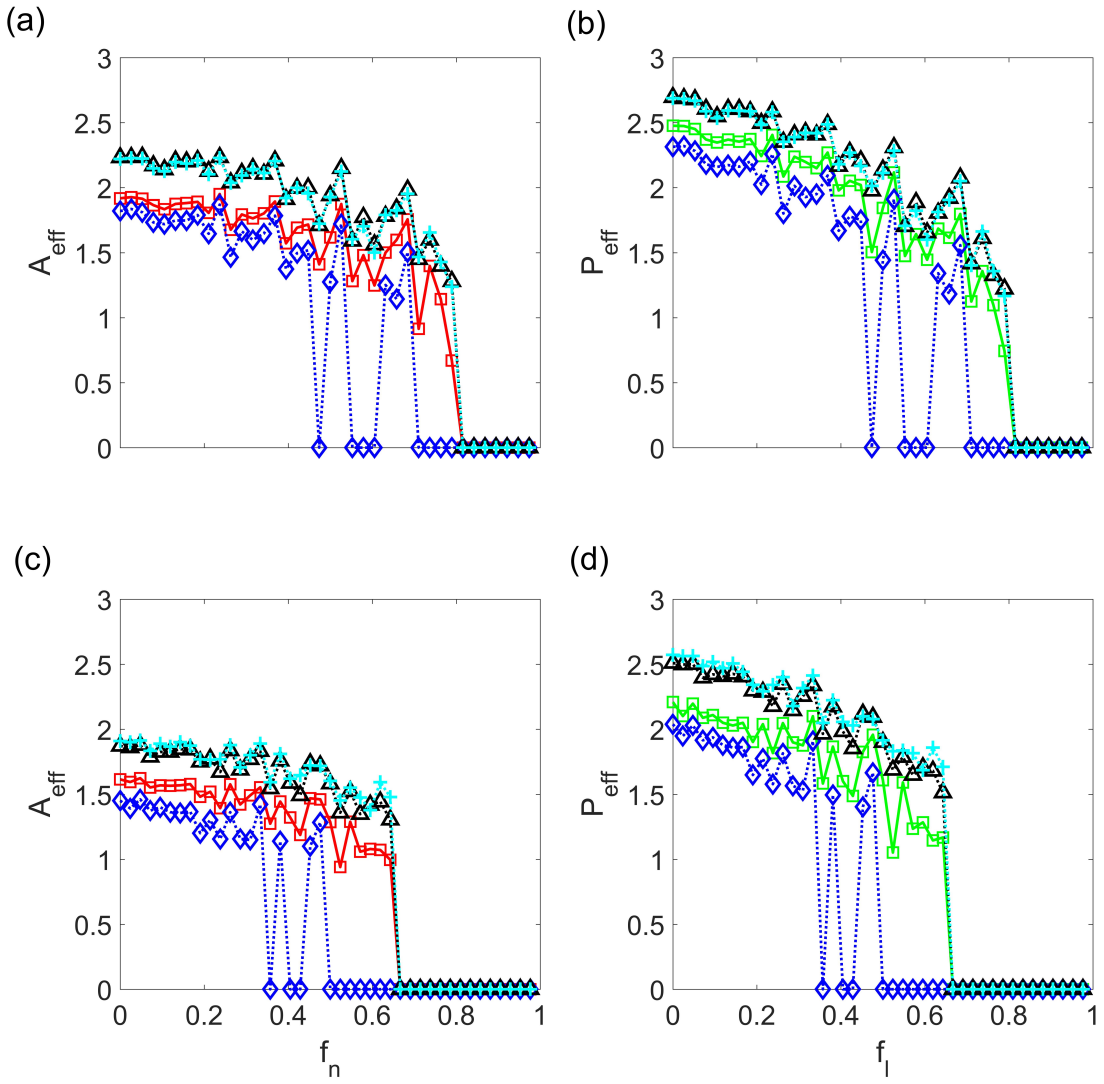

fig. S2. Representative resilient functions in systems that exhibit a tipping point. For networks A [panels (a,b)] and B [panels (c,d)], examples of resilient functions of pollinator abundance [panels (a,c)] versus f_n, the fraction of removed pollinators, and plant abundance [panels (b,d)] versus f_l, the fraction of removed mutualistic links corresponding to the value of f_n in panels (a,c). The curves with squares are from the original networked system, while the curves with diamonds, triangles, and crosses are the corresponding individual resilient functions from reduced 2D model with averaging methods 1-3, respectively. Before f_n (or f_l for plants) approaches unity, total collapse of the system can occur past a tipping point, at which the species abundances effectively become zero. The parameters are $h = 0.2$, $t = 0.5$, $\beta_{ii}^{(A)} = \beta_{ii}^{(P)} = 1$, $\alpha_i^{(A)} = \alpha_i^{(P)} = -0.3$, $\mu_A = \mu_P = 0.0001$, $\gamma_0 = 1$, and $\kappa = 0$.

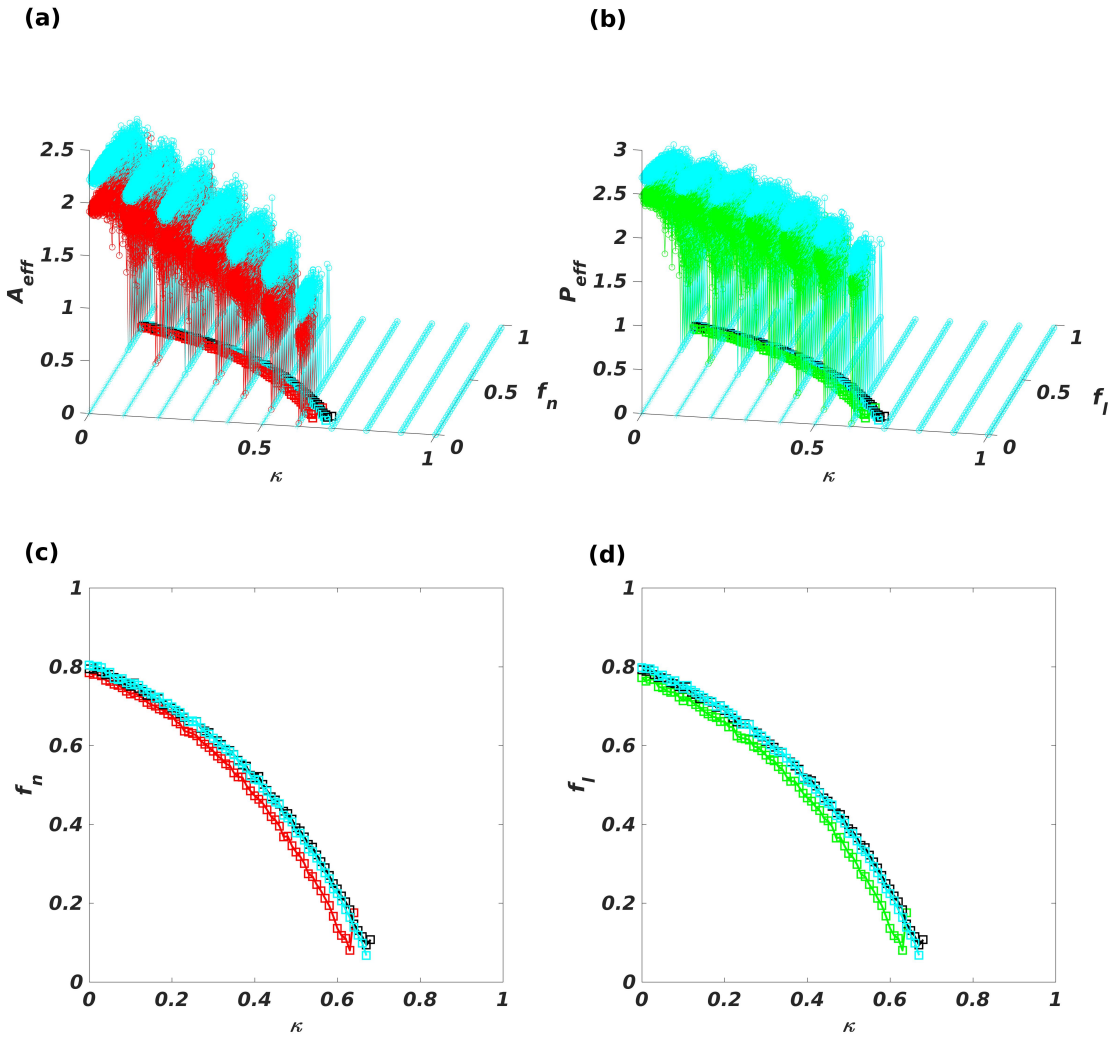

fig. S3. Tipping point in two-dimensional parameter space for network A. Panels (a,c) and (b,d) are for the pollinators and plants, respectively. The circles and asterisks in panels (a) and (b) are results from the original model with $\delta\kappa = 0.1$, and the cyan curves are results from the reduced model obtained through the eigenvector weighted averaging method. The circles and asterisks curves in both panels indicate the cases where the initial species abundance is high (10) and low (0.01), respectively. Each point on the red squared curve represents the ensemble averaged critical f_n value (with 100 realizations) for a fixed value of κ, where $\delta\kappa = 0.01$. The black and cyan square curves are the average abundances predicted by the reduced models with degree-weighted and eigenvector weighted averaging, respectively. Panels (c,d) indicate the critical curve of tipping point in the parameter plane. For each value of f_n (or, equivalently, f_l) and κ, 100 network realizations are used. Other parameters are the same as those in Fig. 4 in the main text. These results indicate that our reduced model with the weighted averaging method can accurately predict the tipping point in the two-dimensional parameter space.

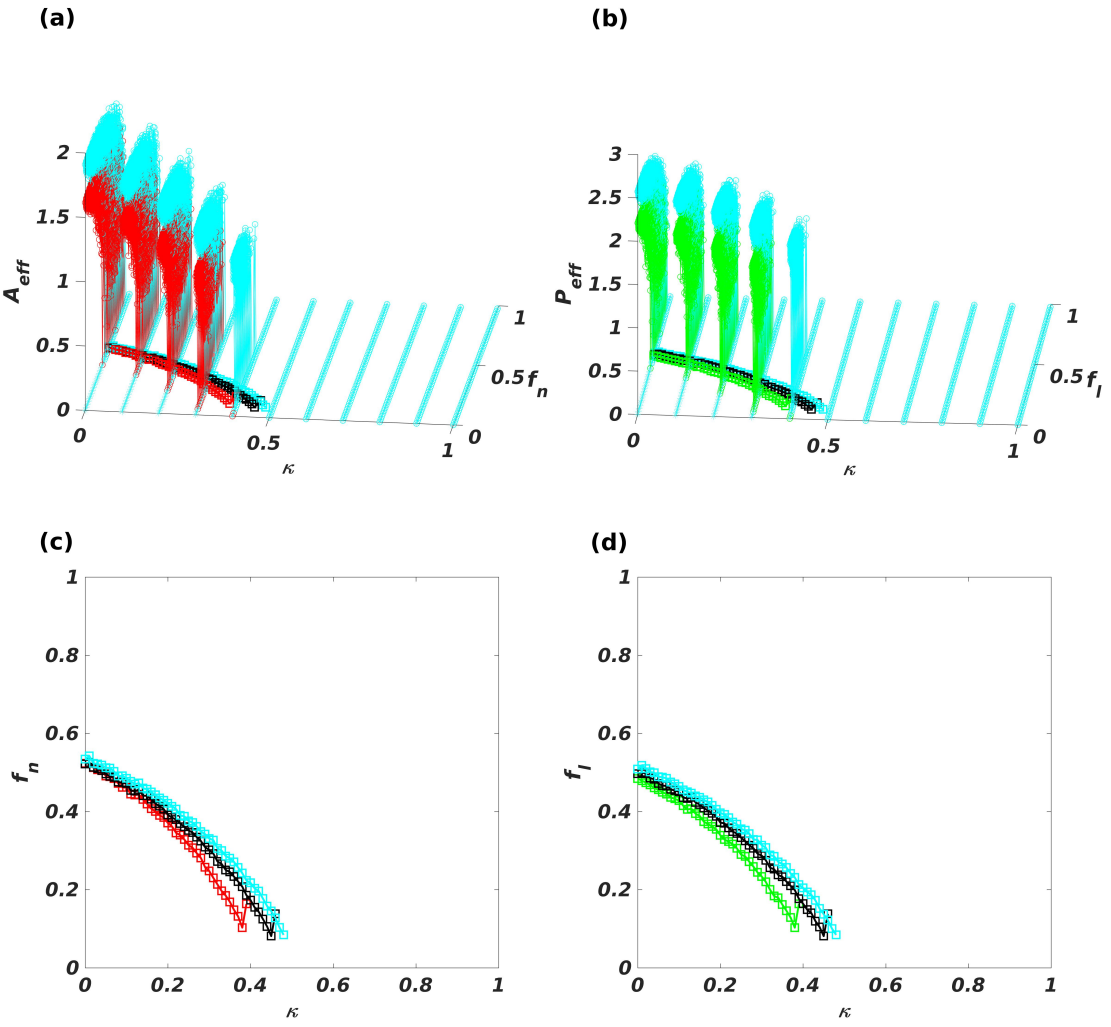

fig. S4. Tipping point in two-dimensional parameter space for network B. Panels (a,c) and (b,d) are for the pollinators and plants, respectively. The circles and asterisks in panels (a) and (b) are results from the original model with $\delta\kappa = 0.1$, and the cyan curves are results from the reduced model obtained through the eigenvector weighted averaging method. The circles and asterisks curves in both panels indicate the cases where the initial species abundance is high (10) and low (0.01), respectively. Each point on the red squared curve represents the ensemble averaged critical f_n value (with 100 realizations) for a fixed value of κ, where $\delta\kappa = 0.01$. The black and cyan square curves are the average abundances predicted by the reduced models with degree-weighted and eigenvector weighted averaging, respectively. Panels (c,d) indicate the critical curve of tipping point in the parameter plane. For each value of f_n (or, equivalently, f_l) and κ, 100 network realizations are used. Other parameters are the same as those in Fig. 9 in the main text. These results indicate that our reduced model with the weighted averaging method can accurately predict the tipping point in the two-dimensional parameter space.

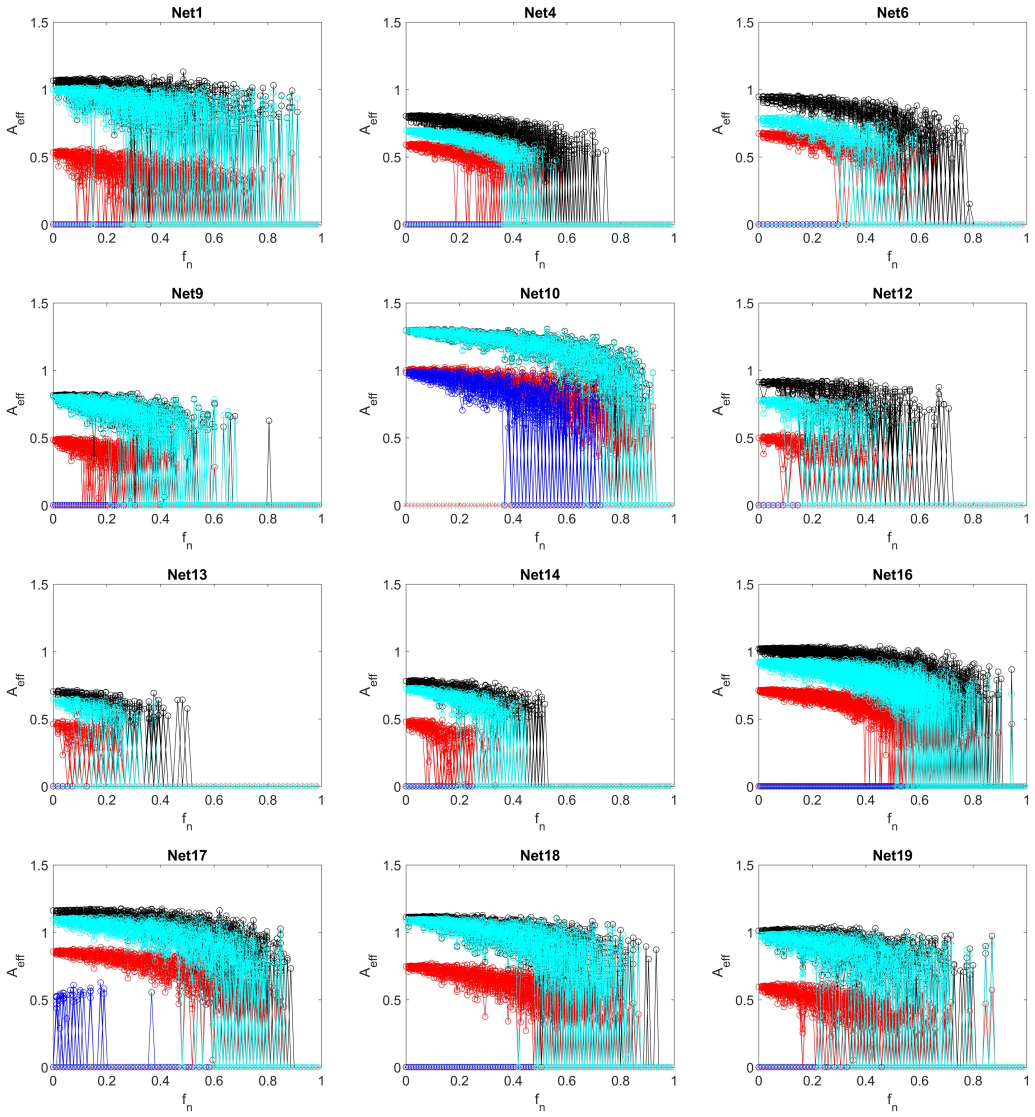

fig. S5. Predicting tipping point for one dozen representative mutualistic networks from the set of 59 real networks. The red curves are the average pollinator and plant abundance, respectively, from the original system. The blue, black and cyan curves in all the panels are the abundances from the reduced 2D system using the averaging methods 1-3, respectively. The circles asterisks in all panels correspond to cases where the initial abundance value relatively high (10) and low (0.01), respectively. For each value of f_n (or f_l), results from 100 statistical realizations are displayed. The model parameters are $h = 0.4$, $t = 0.5$, $\beta_{ii}^{(A)} = \beta_{ii}^{(P)} = 1$, $\alpha_i^{(A)} = \alpha_i^{(P)} = -0.3$, $\mu_A = \mu_P = 0.0001$, and $\gamma_0 = 1$.

SI Appendix Note 1: Derivation of the 2D reduced model

Our dimension reduction process is based on the following two assumptions. Firstly, the decay parameters for all the pollinators have an identical value: $\kappa_i \equiv \kappa$. There is a qualitative correspondence between κ and the state of the environment in that a deteriorating environment for species implies an increased value of κ. Thus, as κ is increased, extinction of species can occur. The tipping point of the system is defined as the critical value of κ beyond which all species are extinct. Secondly, for structural perturbation, we assume that pollinators die from the mutualistic network one after another as a result of increasingly deteriorating environment. As the fraction of disappearing pollinators is increased, a total collapse of all the species can occur. Due to the removal of the mutualistic links, a complete collapse of the plant species can occur at the same time, defining a tipping point of the system as a result of structural perturbation on the network.

Given a high-dimensional mutualistic network, the reduced dynamical system contains two coupled ODEs: one for the pollinators and another for the plants. The basic idea of dimension reduction is to characterize the "information" about the network topology by an effective dynamical parameter. The process consists of the following three steps.

Firstly, we obtain the effective (average) abundances of the plants and the pollinators. From Eq. (1) in the main text, we have

$$\alpha_i^{(P)} P_i \cong \alpha P_{eff} \ \text{ and } \ \alpha_i^{(A)} A_i \cong \alpha A_{eff}, \tag{S1}$$

where P_{eff} and A_{eff} the effective abundances of the plants and the pollinators, respectively. Secondly, since species do not out-compete each other when mutualistic partners are absent [1], intraspecific competitions can be assumed to be stronger than the interspecific competitions, leading to

$$\beta_{ii}^{(P)} \gg \beta_{ij}^{(P)} \ \text{ and } \ \beta_{ii}^{(A)} \gg \beta_{ij}^{(A)}. \tag{S2}$$

For simplicity, we can totally neglect the interspecific competitions. The terms describing the species competitions in Eq. (1) in the main text can then be written as

$$\sum_{j=1}^{S_P} \beta_{ij}^{(P)} P_i P_j \approx \beta_{ii}^{(P)} P_i^2 \cong \beta P_{eff}^2 \ \text{ and } \ \sum_{j=1}^{S_A} \beta_{ij}^{(A)} A_i A_j \approx \beta_{ii}^{(A)} A_i^2 \cong \beta A_{eff}^2. \tag{S3}$$

To incorporate interspecific competitions into the model, we write the species competition terms in Eq. (1)

in the main text as

$$\sum_{j=1}^{S_P} \beta_{ij}^{(P)} P_i P_j \cong \frac{\sum_{i=1}^{S_P}\sum_{j=1}^{S_P} \beta_{ij}^{(P)}}{\sum_{i=1}^{S_P} 1} P_{eff}^2 = \beta P_{eff}^2, \tag{S4}$$

$$\sum_{j=1}^{S_A} \beta_{ij}^{(A)} A_i A_j \cong \frac{\sum_{i=1}^{S_A}\sum_{j=1}^{S_A} \beta_{ij}^{(A)}}{\sum_{i=1}^{S_A} 1} A_{eff}^2 = \beta A_{eff}^2.$$

Thirdly, for effectively representing the mutualistic interactions in the network, we first calculate the mutualistic strength of every single species, as follows:

$$\sum_{j=1}^{S_P} \gamma_{ij}^{(A)} P_j = \sum_{j=1}^{S_P} \frac{\gamma_0}{k_{A_i}^t} \varepsilon_{ij} P_j \cong \gamma_0 k_{A_i}^{(1-t)} P_{eff} \text{ and } \sum_{j=1}^{S_A} \gamma_{ij}^{(P)} A_j = \sum_{j=1}^{S_A} \frac{\gamma_0}{k_{P_i}^t} \varepsilon_{ij} A_j \cong \gamma_0 k_{P_i}^{(1-t)} A_{eff}. \tag{S5}$$

We then calculate the average mutualistic interacting strength in the system. There can be a variety of choices as to how the averaging process is carried out. Here we consider three methods: unweighted, degree weighted, and eigenvector weighted. For the unweighted method, we have

$$\langle \gamma_P \rangle = \frac{\sum_{i=1}^{S_P} \gamma_0 k_{P_i}^{1-t}}{\sum_{i=1}^{S_P} 1} \text{ and } \langle \gamma_A \rangle = \frac{\sum_{i=1}^{S_A} \gamma_0 k_{A_i}^{1-t}}{\sum_{i=1}^{S_A} 1}. \tag{S6}$$

For the degree-weighted method, we have

$$\langle \gamma_P \rangle = \frac{\sum_{i=1}^{S_P} \gamma_0 k_{P_i}^{1-t} \times k_{P_i}}{\sum_{i=1}^{S_P} k_{P_i}} \text{ and } \langle \gamma_A \rangle = \frac{\sum_{i=1}^{S_A} \gamma_0 k_{A_i}^{1-t} \times k_{A_i}}{\sum_{i=1}^{S_A} k_{A_i}}. \tag{S7}$$

Where k_{P_i} and k_{A_i} are the numbers of mutualistic interacting links associated with P_i and A_i, respectively. For the eigenvector-weighted method, we calculate the averaging quantities for pollinators and plants based on the eigenvector associated with the largest eigenvalue of the respective projection networks. Let M_P and M_A be the projection matrices of the plants and pollinators, respectively. We have

$$M_P = M^T \times M,\ V_P = \text{eigenvector}(M_P) \text{ and } M_A = M \times M^T,\ V_A = \text{eigenvector}(M_A), \tag{S8}$$

where M is the $m \times n$ matrix characterizing the original bipartite network with m and n being the numbers of pollinators and plants, respectively), V_P and V_A are the components of the eigenvector associated with the

largest eigenvalue of M_P and M_A, respectively. We then get

$$\langle \gamma_P \rangle = \frac{\sum_{i=1}^{S_P} \gamma_0 k_{P_i}^{1-t} \times V_P^{(i)}}{\sum_{i=1}^{S_A} V_P^{(i)}} \text{ and } \langle \gamma_A \rangle = \frac{\sum_{i=1}^{S_A} \gamma_0 k_{A_i}^{1-t} \times V_A^{(i)}}{\sum_{i=1}^{S_A} V_A^{(i)}}, \tag{S9}$$

where $V_P^{(i)}$ and $V_A^{(i)}$ are the i^{th} component of V_P and V_A, respectively.

SI Appendix Note 2: Description of the 59 real mutualistic networks

Index	# Pollinators	# Plants	Linkage	Network Location
1	101	84	0.04	Cordón del Cepo, Chile
2	64	43	0.07	Cordón del Cepo, Chile
3	25	36	0.09	Cordón del Cepo, Chile
4	102	12	0.14	Central New Brunswick, Canada
5	275	96	0.03	Pikes Peak, Colorado, USA
6	61	17	0.14	Hickling, Norfolk, UK
7	36	16	0.15	Shelfanger, Norfolk, UK
8	38	11	0.25	Tenerife, Canary Islands
9	118	24	0.09	Latnjajaure, Abisko, Sweden
10	76	31	0.19	Zackenberg
11	13	14	0.29	Mauritius Island
12	55	29	0.09	Garajonay, Gomera, Spain
13	56	9	0.2	KwaZulu-Natal region, South Africa
14	81	29	0.08	Hazen Camp, Ellesmere Island, Canada
15	666	131	0.03	DaphnÃ, Athens, Greece
16	179	26	0.09	Doñana National Park, Spain
17	79	25	0.15	Bristol, England
18	108	36	0.09	Hestehaven, Denmark
19	85	40	0.08	Snowy Mountains, Australia
20	91	20	0.1	Hazen Camp, Ellesmere Island, Canada
21	677	91	0.02	Ashu, Kyoto, Japan
22	45	21	0.09	Laguna Diamante, Mendoza, Argentina

Table S1 – continued from previous page

Index	# Pollinators	# Plants	Linkage	Network Location
23	72	23	0.08	Rio Blanco, Mendoza, Argentina
24	18	11	0.19	Melville Island, Canada
25	44	13	0.25	North Carolina, USA
26	54	105	0.04	Galapagos
27	60	18	0.11	Arthur's Pass, New Zealand
28	139	41	0.07	Cass, New Zealand
29	118	49	0.06	Craigieburn, New Zealand
30	53	28	0.07	Guarico State, Venezuela
31	49	48	0.07	Canaima Nat. Park, Venezuela
32	33	7	0.28	Brownfield, Illinois, USA
33	34	13	0.32	Ottawa, Canada
34	128	26	0.09	Chiloe, Chile
35	36	61	0.08	Morant Point, Jamaica
36	12	10	0.25	Flores, AÃores Island
37	40	10	0.18	Hestehaven, Denmark
38	42	8	0.24	Hestehaven, Denmark
39	51	17	0.15	Tenerife, Canary Islands
40	43	29	0.09	Windsor, The Cockpit Country, Jamaica
41	43	31	0.11	Syndicate, Dominica
42	6	12	0.35	Puerto Villamil, Isabela Island, Galapagos
43	82	28	0.11	Hestehaven, Denmark
44	609	110	0.02	Amami-Ohsima Island, Japan
45	26	17	0.14	Uummannaq Island, Greenland
46	44	16	0.39	Denmark
47	186	19	0.12	Isenbjerg

Table S1 – continued from previous page

Index	# Pollinators	# Plants	Linkage	Network Location
48	236	30	0.09	Denmark
49	225	37	0.07	Denmark
50	35	14	0.18	Tenerife, Canary Islands
51	90	14	0.13	Nahuel Huapi National Park, Argentina
52	39	15	0.16	Tundra, Greenladn
53	294	99	0.02	Mt. Yufu, Japan
54	318	113	0.02	Kyoto City, Japan
55	195	64	0.03	Nakaikemi marsh, Fukui Prefecture, Japan
56	365	91	0.03	Mt. Kushigata, Yamanashi Pref., Japan
57	883	114	0.02	Kibune, Kyoto, Japan
58	81	32	0.12	Parc Natural del Cap de Creus
59	13	13	0.42	Parque Nacional do Catimbau

table S1. The 59 real pollinator-plant networks are from web-of-life (http://www.web-of-life.es). For each network, the linkage is normalized with respect to the corresponding fully connected (all-to-all) network for which the linkage is 100%.

SI Appendix Note 3: Steady state solutions of the pollinator and plant abundances

The steady state solutions of the reduced model can be obtained by setting $dP_{eff}/dt = 0$ and $dA_{eff}/dt = 0$, which gives

$$f(P', A') = \alpha P' - \beta P'^2 + \frac{\langle\gamma_P\rangle A'}{1 + h\langle\gamma_P\rangle A'} P' + \mu = 0, \tag{S10}$$
$$g(P', A') = \alpha A' - \beta A'^2 + \frac{\langle\gamma_A\rangle P'}{1 + h\langle\gamma_A\rangle P'} A' + \mu = 0,$$

where A' and P' denote the effective pollinator and plant abundances in the steady state, respectively. The Jacobian matrix evaluated at a steady-state solution is

$$J = \begin{Bmatrix} \alpha - 2P'\beta + \frac{h\langle\gamma_P\rangle A'}{1+h\langle\gamma_P\rangle A'} & -\frac{h^2\langle\gamma_P\rangle^2 A'P'}{(1+h\langle\gamma_P\rangle A')^2} + \frac{h\langle\gamma_P\rangle P'}{1+h\langle\gamma_P\rangle A'} \\ -\frac{h^2\langle\gamma_A\rangle^2 A'P'}{(1+h\langle\gamma_A\rangle P')^2} + \frac{h\langle\gamma_A\rangle A'}{1+h\langle\gamma_A\rangle P'} & \alpha - 2A'\beta - \kappa + \frac{h\langle\gamma_A\rangle p'}{1+h\langle\gamma_A\rangle P'} \end{Bmatrix}. \tag{S11}$$

We solve Eq. (S10) to get

$$\begin{aligned} P' &= \frac{1}{-2\beta}[-(\alpha + \frac{\langle\gamma_P\rangle A'}{1 + h\langle\gamma_P\rangle A'}) \pm ((\alpha + \frac{\langle\gamma_P\rangle A'}{1 + h\langle\gamma_P\rangle A'})^2 + 4\beta\mu)^{1/2}], \\ A' &= \frac{1}{-2\beta}[-(\alpha - \kappa + \frac{\langle\gamma_A\rangle P'}{1 + h\langle\gamma_A\rangle P'}) \pm ((\alpha - \kappa + \frac{\langle\gamma_A\rangle P'}{1 + h\langle\gamma_A\rangle P'})^2 + 4\beta\mu)^{1/2}]. \end{aligned} \tag{S12}$$

The physically meaningful solutions of P' and A' have positive values. Because of the parameter setting $|\alpha| \gg \mu = 0.0001$, we have

$$\beta\mu \ll |\alpha + \frac{\langle\gamma_P\rangle A'}{1 + h\langle\gamma_P\rangle A'}| \text{ or } |\alpha - \kappa + \frac{\langle\gamma_A\rangle P'}{1 + h\langle\gamma_A\rangle P'}|.$$

The approximate solutions of P' and A' are then given by

$$\begin{aligned} P' &\approx \frac{1}{-2\beta}[-(\alpha + \frac{\langle\gamma_P\rangle A'}{1 + h\langle\gamma_P\rangle A'}) \pm (|\alpha + \frac{\langle\gamma_P\rangle A'}{1 + h\langle\gamma_P\rangle A'}| + 2\beta\mu)], \\ A' &\approx \frac{1}{-2\beta}[-(\alpha - \kappa + \frac{\langle\gamma_A\rangle P'}{1 + h\langle\gamma_A\rangle P'}) \pm (|\alpha - \kappa + \frac{\langle\gamma_A\rangle P'}{1 + h\langle\gamma_A\rangle P'}| + 2\beta\mu)]. \end{aligned} \tag{S13}$$

For $\alpha + (\langle\gamma_P\rangle A')/(1 + h\langle\gamma_P\rangle A') > 0$, we have the following two approximate solutions of P':

$$\begin{aligned} P'_1 &\approx -\mu, \\ P'_2 &\approx \frac{1}{\beta}(\alpha + \frac{\langle\gamma_P\rangle A'}{1 + h\langle\gamma_P\rangle A'}), \end{aligned} \tag{S14}$$

where P'_1 corresponds to the result in Eq. (S13) with the $+$ sign and P'_2 with the $-$ sign. The corresponding solutions A'_1 and A'_2 can be obtained accordingly.

For $\alpha + (\langle\gamma_P\rangle A')(1 + h\langle\gamma_P\rangle A') < 0$, we have

$$\begin{aligned} P_1' &\approx \frac{1}{\beta}(\alpha + \frac{\langle\gamma_P\rangle A'}{1 + h\langle\gamma_P\rangle A'}), \\ P_2' &\approx \mu. \end{aligned} \tag{S15}$$

For $\alpha - \kappa + (\langle\gamma_A\rangle P')(1 + h\langle\gamma_A\rangle P') > 0$, we have

$$\begin{aligned} A_1' &\approx -\mu, \\ A_2' &\approx \frac{1}{\beta}(\alpha - \kappa + \frac{\langle\gamma_A\rangle P'}{1 + h\langle\gamma_A\rangle P'}). \end{aligned} \tag{S16}$$

For $\alpha - \kappa + (\langle\gamma_A\rangle P')(1 + h\langle\gamma_A\rangle P') < 0$, we have

$$\begin{aligned} A_1' &\approx \frac{1}{\beta}(\alpha - \kappa + \frac{\langle\gamma_A\rangle P'}{1 + h\langle\gamma_A\rangle P'}), \\ A_2' &\approx \mu. \end{aligned} \tag{S17}$$

SI Appendix References

[1] Egbert H van Nes and Marten Scheffer. Large species shifts triggered by small forces. *Amer. Nat.*, 164(2):255–266, 2004.